15

Assessment of Cardiac and Thoracic Masses

Jabi E. Shriki, Patrick M. Colletti, and William D. Boswell Jr

Overview

Excellent spatial and contrast resolution make cardiovascular computed tomographic angiography (CCTA) an ideal method for the detection and evaluation of cardiac masses and masses adjacent to the heart. Suspended respiration and cardiac gating techniques employed with CCTA enhance delineation of planes between masses and normal structures. While many cardiac masses are well demonstrated with nongated CT, two approaches to cardiac gating may be applied: prospective ECG triggering and retrospective ECG gating [1]. The ability to freeze cardiac motion enables clearer evaluation of tissue attenuation and enhancement characteristics of normal myocardium and of masses.

Precontrast imaging may help to identify features of masses such as calcifications, which appear as foci of punctuate or coarse hyperattenuation, typically in the range of 130 Hounsfield units (HU), and hemorrhage, which may have a more modest and ill-defined hyperattenuation relative to normal myocardium. Precontrast low attenuation may be helpful for characterizing myxomas or cystic features of masses. Comparison of pre- and postcontrast images is also useful in quantifying the amount of enhancement. Tumor enhancement may occur in a later phase and may not be well-seen in the arterial phase, during which CCTA is usually performed; this is however, dependent on the degree of vascularity within the tumor. However, optimal opacification of the left atrium and left ventricle will allow clear delineation of masses that extend into the chambers of the left heart. The amount of iodinated contrast agent required for satisfactory CT evaluation of cardiac masses depends on patient mass, with 0.5–1.0 g of iodine per kilogram body mass as the usual dose [2]. Using standard low-osmolality contrast agents with concentrations of 300–400 mg iodine/mL, typically 100 mL of contrast agent is administered at 4–5 mL/s via a programmable injector system. This is followed by a bolus flush of 50 mL of normal saline [3].

Timing the CT image acquisition to the contrast agent bolus arrival for most left atrial and left ventricular masses is identical to timing used for coronary artery CT examinations [4]. Optimal left atrial appendage enhancement may, however, be somewhat difficult, since the left atrial appendage may opacify somewhat more slowly or heterogeneously. In addition, there may be considerable variability in circulation time from patient to patient, particularly in patients with cardiac tumors or thrombi. The time between peripheral contrast injection and appearance of contrast in the aorta can be determined using a small volume test contrast agent bolus of 20 mL and rapid, repeated imaging of a single transaortic plane [5]. Alternatively, with bolus tracking, a HU threshold may be set such that the volume acquisition is triggered to begin once a certain HU value is detected in the ascending aorta. A uniform, programmed injection requires 10–25 s for delivery of intravenous contrast agent and up to 50 additional seconds for the saline flush. One potential pitfall in employing automatic bolus detection in cardiac masses is that it is possible to inadvertently place the bolus detection region-of-interest (ROI) within a chamber or a vessel which contains internal thrombus or tumor. Such an error results may result in failure to detect the bolus as shown in (Figure 15.1).

Opacification of the right heart with contrast may be more challenging. Without appropriate acquisition timing for right heart visualization, there may be insufficient contrast for delineation of right atrial and right ventricular endocardial borders. Excessive contrast within the right heart may result in streaking and obscuration of subtle masses. Optimal timing and technique for right heart examination usually differs from that used for routine CCTA. In most patients, optimal right ventricular opacification is achieved by placing the ROI for bolus tracking in the main pulmonary artery. Right ventricular delineation in congenital heart disease with transposition or other abnormal great vessel relationships requires some a priori
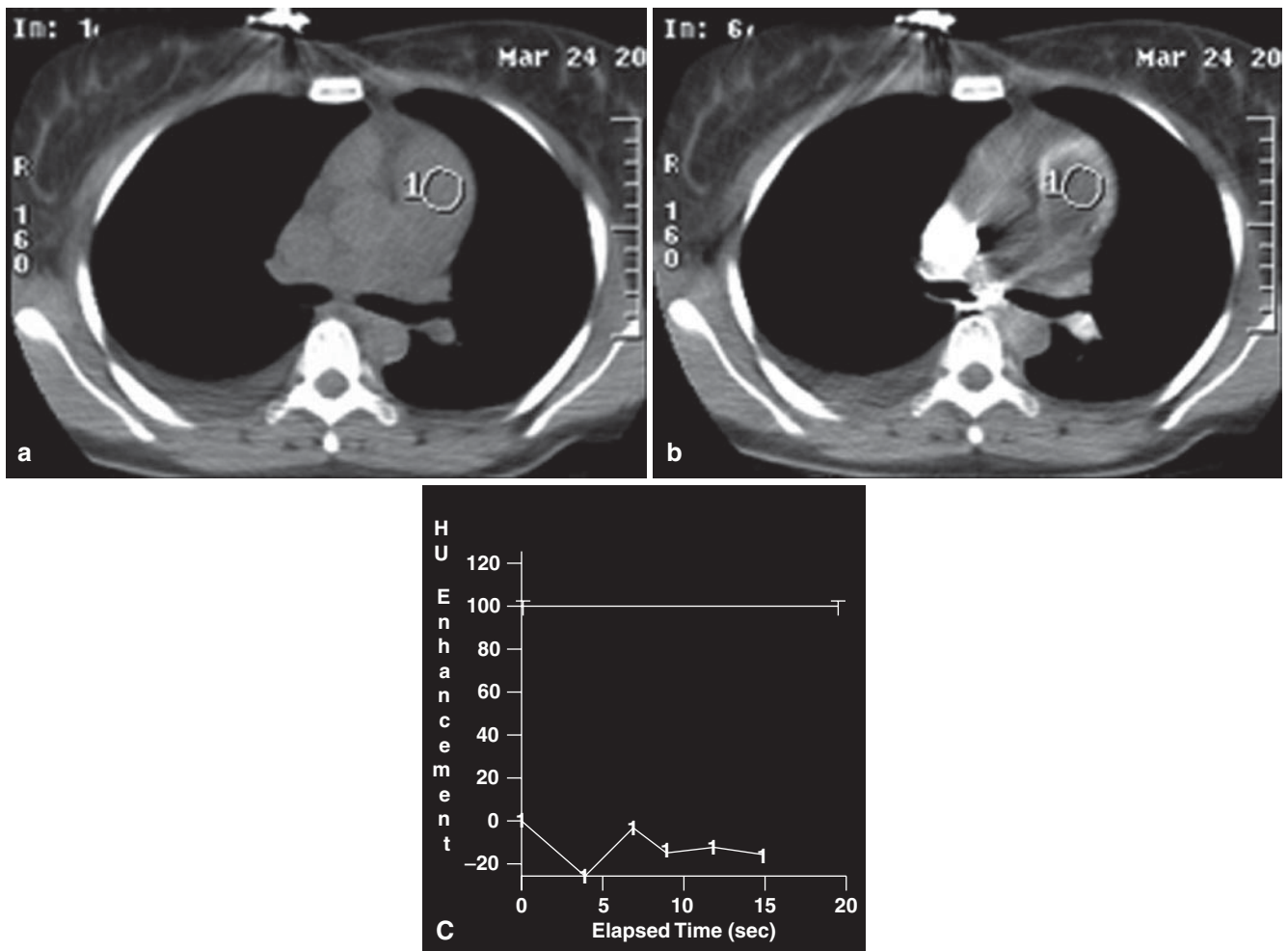
Figure 15.1. (**a**, **b**) Pitfall of automated bolus detection. Automatic bolus detection fails due to tumor replacing the blood pool in the selected region-of-interest (ROI) in the main pulmonary artery. The enhancement curve (**c**) shows that the preset attenuation threshold is not met, due to placement of the ROI in the mass within the pulmonary artery.

knowledge of the anatomy and relevant surgical history to select the correct region for timing prescription. When opacification of multiple chambers is needed, more complex injection protocols can be utilized with multiphasic contrast administration, including injection of mixtures of saline and contrast [6].

One advantage cardiac magnetic resonance imaging (CMR) holds over cardiac CT for cardiac masses is the ability to obtain excellent contrast for both the right ventricle and left ventricle in the same examination due to the ability to image the heart in multiple phases of contrast administration, with no radiation dose. Further investigations are needed to determine how to reliably achieve sufficient contrast in both ventricles with CCTA.

Clinical [7–19] and imaging [20–28] features of cardiac masses are summarized in Tables 15.1–15.4.

Table 15.1. Benign cardiac neoplasms

	Location	Features
Myxoma (40% of all benign tumors) (Figure 15.16)	LA septum 75%; RA 18%; ventricles 7%; multiple 5%	10% calcified; frequent systemic emboli; may protrude through mitral valve during diastole
Fibroelastoma	Arise from valves; project into aorta or MPA	Derived from endocardium; may be multiple; often an incidental finding at surgery
Lipoma	Varies	Encapsulated adipose tissue (fat attenuation); asymptomatic; negative CT density; 25% are multiple; consider tuberous sclerosis; should not be confused with fat in paracardiac folds
Lipomatous hypertrophy	Atrial septum; protrudes into RA	Fat attenuation
Fibroma	Myocardium	Well-delineated, calcified; enhance minimally
Hemangioma	Myocardium	Calcifications; delayed enhancement
Lymphangioma	Myocardium	Diffuse proliferation; minimally enhancing
Paraganglioma, dysembryoma, pheochromocytoma	Paracardiac; AV groove	Sympathetic plexus; hyper-enhancing; correlate with urinary catecholamines; alpha-and beta-blockade for surgery
Teratoma	Pericardial; attach to the aorta or PAroots	Multicystic; frequently calcify; moderate enhancement

Table 15.2. Cystic cardiac masses

	Location	Features
Pleuro-pericardial cyst	75% in right paracardiac angle	Asymptomatic (avascular/calcified); unilocular, sharply marginated, 20–40 HU; may communicate with pericardium; change shape with body position
Echinococcal cysts	Myocardial or pericardial	(Avascular/calcific rim); nearly always also in liver, lung, eyes, brain
Tuberculoma	Myocardial or pericardial	Calcified; constrictive pericarditis
Hematoma	Posterior recesses at the aortic root or left atrium	Acutely hyper-dense; may calcify; traumatic or postsurgical
Thrombosed coronary aneurysm	Course of coronary arteries	Calcified rim; thrombus

Table 15.3. Malignant cardiac tumors

	Location	Features
Metastasis (20×as common as primary tumor) (Figure 15.2)	Pericardial; intravascular; intramyocardial	Seen in 10% of end-stage cancers; lung (36%), breast (7%), esophagus (6%); lymphoma, melanoma, Kaposi's sarcoma, leukemia (20%); modes of dissemination: direct or lymphatic; hematogenous; direct venous extension (pulmonary veins or inferior vena cava)
Lung, breast, melanoma, sarcoma, leukemia, thyroid, kidney	Pericardial; direct or lymphatic; hematogenous; direct venous extension	Lung cancer may extend to the left atrium along the pulmonary veins
Renal, urothelial, hepatocellular, adrenal, retroperitoneal sarcoma	Extend up the inferior vena cava to the right atrium	Enhancing intravascular mass; primary tumor identified
Lymphoma	Pericardium; myocardium; commonly basal in location	May infiltrate epicardial fat; 50% associated with HIV
Angiosarcoma (Figure 15.1)	Pericardium; RV, RA, myocardium	Angiosarcoma of the pericardium or right ventricle is most common; poor prognosis; distribution is similar to lymphoma
Osteosarcoma	RA, RV	Ossification
Rhabdomyosarcoma, fibrosarcoma	Myocardium	Most common primary cardiac malignancy in infants and children. Always involves the myocardium; pericardial involvement is typically in the form of nodular masses rather than sheet-like spread
Mesothelioma	Pericardium	Intrapericardial mass; effusions; constrictive physiology

Table 15.4. Other cardiac masses

	Location	Features
Endomyocardial fibrosis	Pericardium; myocardium	Thickened pericardium; thickened myocardium with patchy enhancement restrictive and constrictive physiology
Erdheim-Chester disease (nonlangherans fibrosis)	Pericardium; myocardium	Thickened pericardium; thickened myocardium with patchy enhancement restrictive and constrictive physiology
RA thrombus (Figure 15.12)	Right atrium	Associated with indwelling catheters and devices
RV thrombus	Right ventricle	Associated with severe coagulopathy; dilated cardiomyopathy
LA thrombus (Figure 15.11)	Left atrium	Seen in atrial fibrillation and mitral stenosis; attached to posterior or superior atrial wall; may be calcified
LV thrombus (Figure 15.8)	Left ventricle	Common complication of myocardial infarction (20–40% of anterior MIs); contiguous to akinetic myocardium; most common at the apex
Vegetations	Valves; catheters	EKG-triggered cine views of valves helpful

Interpreting Cardiac Masses: Key Descriptors

Location

Lesion location relative to the heart should be noted and may provide a hint as to the nature of a particular mass. Masses related to the heart itself which are cardiac in origin have a unique differential diagnosis. Masses immediately adjacent to the heart and intimately involving the pericardium should be described as pericardial (Figure 15.2). Masses which are external to the heart should be described as paracardial (within the mediastinum, adjacent to the heart). For lesions that are within the mediastinum, a separate set of diagnostic possibilities should be included in the differential. A full discussion of mediastinal masses, however, is beyond the scope of this text. Although some tumors may violate planes and make identification of the organ of origin difficult, in most cases, cardiac masses, pericardial masses, and mediastinal masses can be separated.

Chamber Involvement

The chamber of origin and location within the chamber should be noted. For example a mass in the left atrium attached along the interatrial septum has a higher chance of being an atrial myxoma. A mass in the left atrial appendage has a higher probability of being a thrombus. Some authors have suggested that, on imaging, metastases are more common in the right heart. However, this could be due to the earlier detection of right heart masses, since the wall of the right ventricle is thinner than the wall of the left ventricle. A mass in the left ventricle may be neoplastic, if it
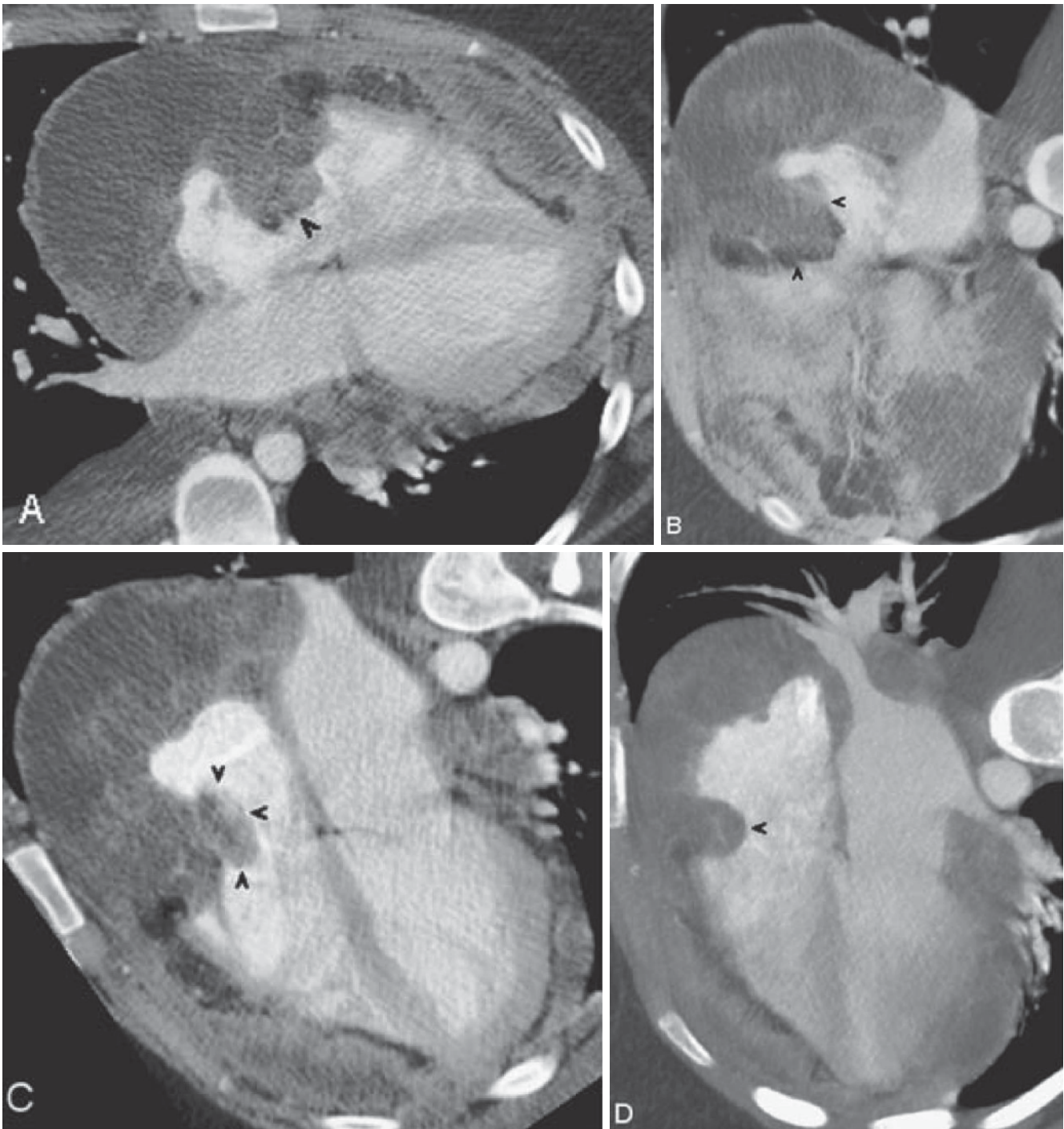
Figure 15.2. Twenty-two-year-old female with a primary pericardial primitive neuroectodermal tumor. Images obtained are obtained as part of a postcontrast nongated CT scan of the chest. Transverse and oblique four-chamber views are shown (**a–d**). In this case, the tumor was causing restriction of cardiac motion, and as a result artifacts due to cardiac motion are mild. There is heavy neoplastic infiltration of the atrioventricular groove with invasion of the right atrium and ventricle (*black arrowheads*).

is felt to be arising from the wall. A mass at the apex of the left ventricle, which appears separate from the wall, has a higher probability of being a thrombus. Attention should be given to associated wall motion abnormalities or aneurysms. Severe metastatic involvement of the myocardial wall may result in a wall motion abnormality. However, a thrombus may present as a mass closely associated with a wall motion abnormality such as dyskinetic aneurysmal segment. Transiently, thrombi with a peripheral origin,

such as deep vein thrombi, may be seen in the right atrium and right ventricle (Figure 15.3). A mass which arises from the crista terminalis of the right atrium may be a prominent network of Chiari. Elastofibromas are common lesions which occur along the valve surfaces, but are usually small and not well-seen on CCTA. Valvular vegetations may rarely grow to a size where they may mimic a cardiac mass, although this diagnosis should be considered in some cases where a mass is closely related to a valve. An example of
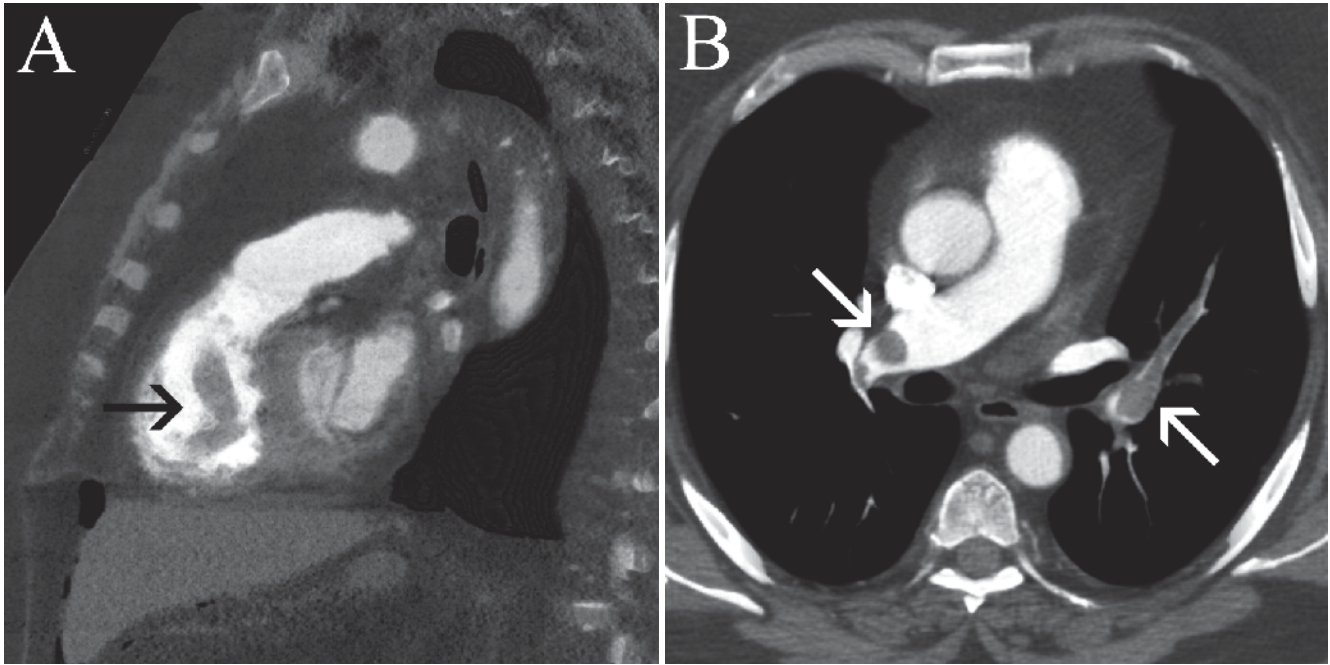
Figure 15.3. Forty-four-year-old female with shortness of breath. The sagittal, minimum intensity projection (MinIP) view shows a vermiform, low-attenuation filling defect (*black arrow*, (**a**)), representing a thrombus in the right ventricle, which had likely migrated from the lower extremities or from the pelvic venous system. MinIP views are useful in demonstrating low attenuation structures, when surrounded by relatively high attenuation. A transverse view on the same study shows multiple, separate pulmonary emboli (*white arrows*, (**b**)).

valvular pathology mimicking a cardiac mass is caseous mitral annular calcification, where an ovoid mass of caseous calcifications develops in close proximity to the mitral annulus as a result of liquefactive necrosis of mitral valvular calcifications (Figure 15.4).
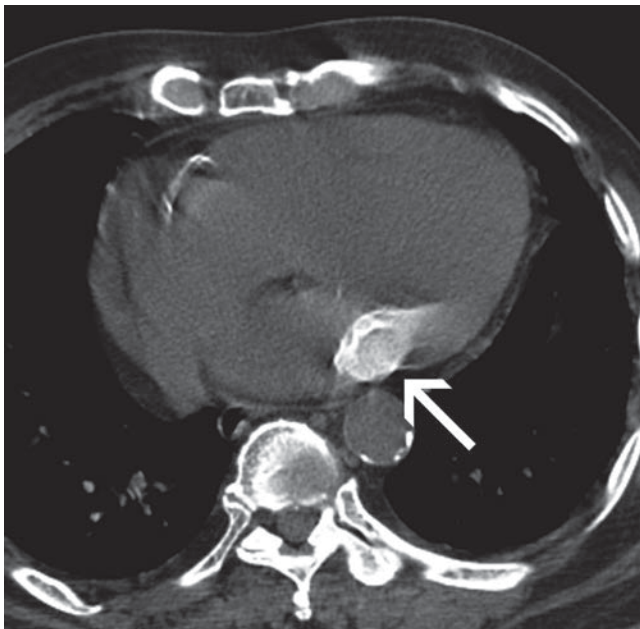

Figure 15.4. Eighty-one-year-old male with caseous mitral annular calcifications. A mass was seen near the region of the mitral annulus on echocardiography. CT was performed for further evaluation. A noncontrast, transverse image shows the classic morphology of caseous mitral annular calcifications, with central homogeneous hyperattenuation representing liquified calcifications and denser, peripheral shell-like calcifications (*white arrow*).

Lesion Morphology

Masses should also be described as intramural (within the myocardial wall) or intracameral (within the cardiac chamber). Metastatic and malignant primary tumors usually have a significant intramural component or a very broad-based attachment to the wall of the myocardium, whereas benign masses are more commonly pedunculated and intracameral, often having a narrow attachment. Although there are exceptions to this rule, this rubric is commonly helpful in identifying pedunculated masses as benign. Thrombi which are adherent to the internal wall of the ventricle are, however, an important exception to this rule. Lesion shape is less helpful as both benign and malignant masses may be lobulated or appear round.

Attenuation

Attenuation can be characterized by HU measurement. Care should be taken to ensure that cardiac gating is adequate as the presence of motion may alter or artifactually elevate measured attenuation. Attenuation values from −100 to −10 HU are generally associated with fatty masses such as intracardiac lipomas or lipomatous hyperplasia of the interatrial septum. Cystic masses will tend to have attenuation values between −10 and 10 HU. Calcifications have an attenuation value of 130 HU or greater. Coarse calcifications may be seen in myxomas, although many other lesions may calcify, including some thrombi and many treated metastases. Attenuation relative to muscle or specifically myocardium is frequently used to describe lesions as hypoattenuating or

hyperattenuating. Frequently, attenuation relative to the blood pool is also described, although it should be noted that patients with anemia may have depressed precontrast attenuation of vascular structures.

Enhancement

Enhancement should be reported with respect to the degree of enhancement and to the phase at which enhancement is seen. Lesions which show no or minimal enhancement are more likely to be benign. This is true of thrombi, which usually show no enhancement. Myxomas usually show minimal or mild postcontrast enhancement. Angiosarcomas,

the most common malignant primary neoplasm of the heart, may have very avid enhancement, to the extent that the borders of these masses may be indistinguishable from contrast within the chamber of the heart. Other neoplastic lesions, including metastases, may show more modest enhancement.

Involvement of Other Vascular Structures

Numerous masses may invade the heart from the great vessels. Tumors of the upper abdomen may grow into the right atrium via the inferior vena cava (Figure 15.5). Hepatocellular carcinoma, adrenocortical carcinoma, and renal
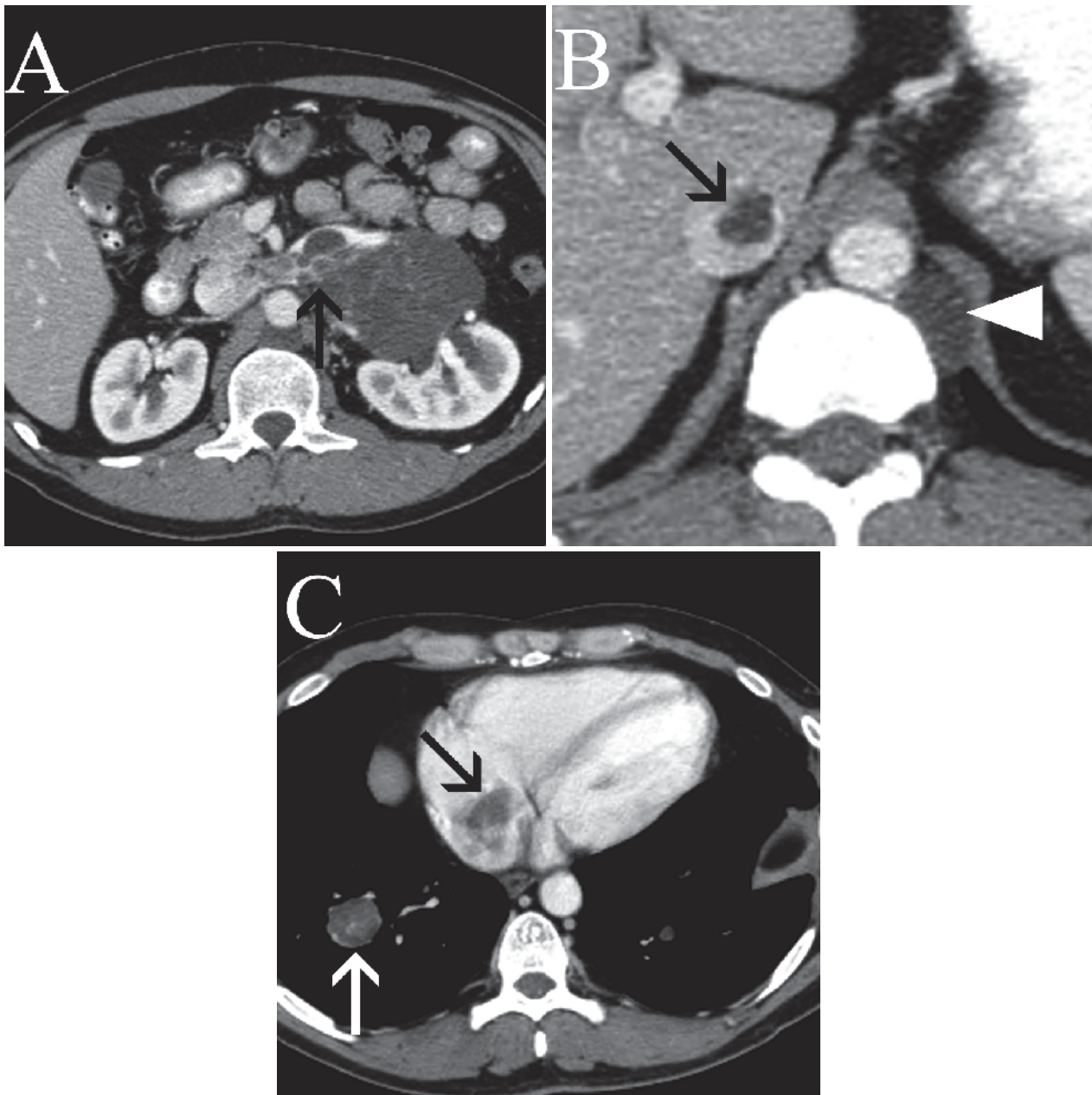

Figure 15.5. Twenty-four-year-old male with retroperitoneal malignant germ cell tumor. Postcontrast CT images are obtained of the abdomen in the portal venous phase and are shown from caudal (**a**) to cranial (**c**). There is extensive left periaortic lymphadenopathy, with invasion of tumor into the left renal vein (*black arrow* on (**a**)). There is also extension of tumor into the IVC and right atrium (*black arrows* on **b**, **c**, respectively). Note other sites of metastatic disease including a right lower lobe metastasis (*white arrow*, (**c**)) and a left retrocrural lymph node (*white arrowhead*, (**b**)). This tumor exhibits a common appearance of metastatic disease from germ cell tumor with low internal attenuation.

cell carcinoma are among the most common tumors of the upper abdomen to invade into the right atrium. Bronchogenic carcinomas may invade into the heart through the pulmonary veins and present as a left atrial mass. Mediastinal tumors and bronchogenic carcinomas that involve the mediastinum may also grow into the heart via the superior vena cava. Tumors of the mediastinum may also grow directly into the heart with external myocardial invasion. Thrombi along catheters may also track along venous structures, most commonly the superior vena cava.

Lesion Number

Multiple lesions are more likely to be due to metastatic disease or to multiple thrombi. Metastatic disease typically appears as multiple lesions in the wall in different locations. Multiple thrombi may be encountered as well, especially when masses are located in characteristic locations, such as the left atrial appendage or the left ventricular apex.

Commonly Encountered Masses

Although a complete discussion of all cardiac masses is beyond the scope of this chapter, familiarity with the most common causes of cardiac masses assists in arriving at the correct diagnosis.

Thrombi

Thrombi are the most common cause of intracardiac masses. On precontrast CT, thrombi may either present as hypoattenuating or hyperattenuating masses, relative to blood pool (Figures 15.6 and 15.7). Attenuation relative to blood pool is influenced by the patient's hematocrit, since more anemic patients will have relatively lower attenuation of blood pool. The degree of attenuation within a thrombus may be dependent on thrombus age. Most thrombi will show no enhancement after administration of contrast. However, some chronic thrombi, described as being more organized, have been reported to have some peripheral enhancement after contrast administration [29]. This is most commonly seen in the setting of chronic thrombi adherent to the wall, and has been reported mostly on magnetic resonance imaging (MRI). On CCTA, essentially no contrast enhancement will be shown within thrombi. In the case of small thrombi, HUs may be elevated after administration of contrast when comparison between pre- and postcontrast CCTA is made, although this is more likely related to pseudoenhancement, whereupon beam hardening effects cause false elevation of attenuation values due to adjacent hyperattenuating structures or contrast. On MRI, thrombi are most commonly dark on all sequences. Thrombi can also be recognized by the characteristic locations in which they occur, including at the left ventricular apex and in the left atrial appendage.

Ventricular thrombi can be recognized by their characteristic location, most commonly at the apex of the left ventricle (Figure 15.8). Morphologically, they may either present as one or many ovoid structures within the chamber or may appear pedunculated (Figure 15.9). Many thrombi may also be flat and layered against the endocardial surface of the left ventricular wall. Association with an underlying wall motion abnormality, such as an area of aneurysm formation or an area of infarction, is also an important hint to the correct diagnosis. Ventricular thrombi
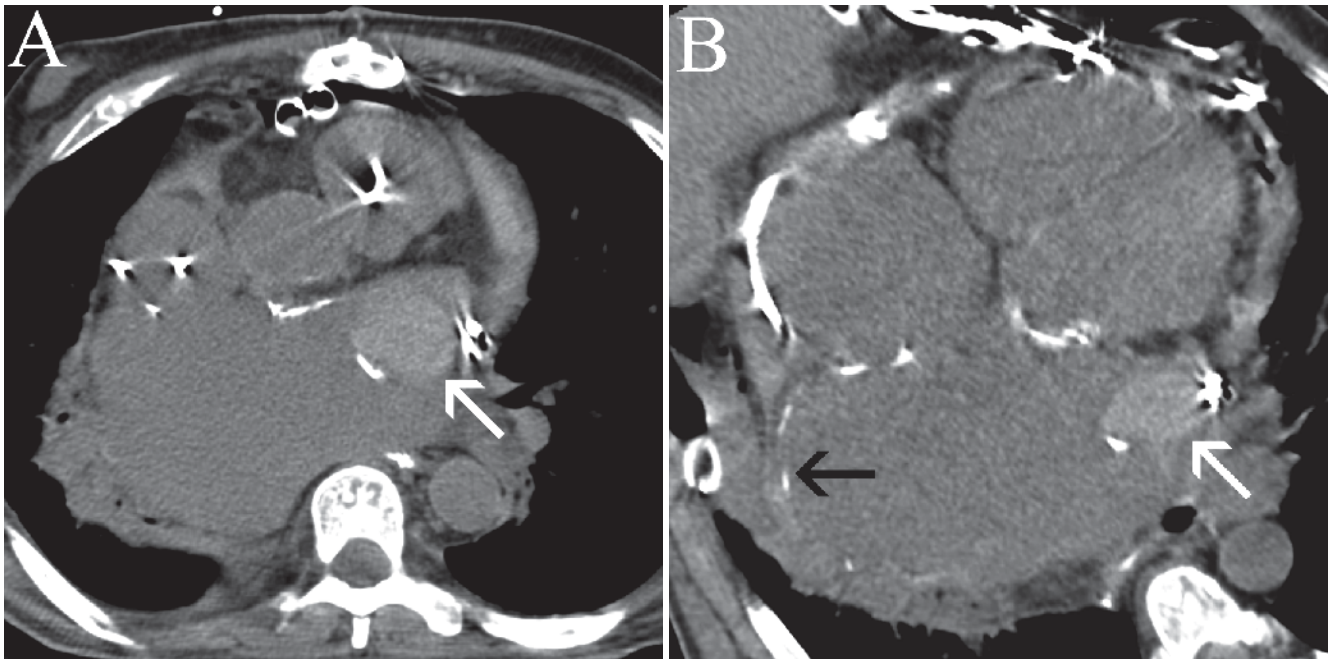

Figure 15.6. Fifty-six-year-old male with rheumatic heart disease and a hyperattenuating left atrial appendage thrombus. Oblique MPR views are shown from a noncontrast scan (**a, b**). A focal mass with hyperattenuation is present in the left atrial appendage, which was also seen on echocardiogram (not shown) and was consistent with an atrial thrombus (*white arrows*). Note the presence of atrial wall calcifications (*black arrow*), which are encountered commonly in the setting of rheumatic heart disease. The left atrium massively enlarged and forms the right heart border (**a**).
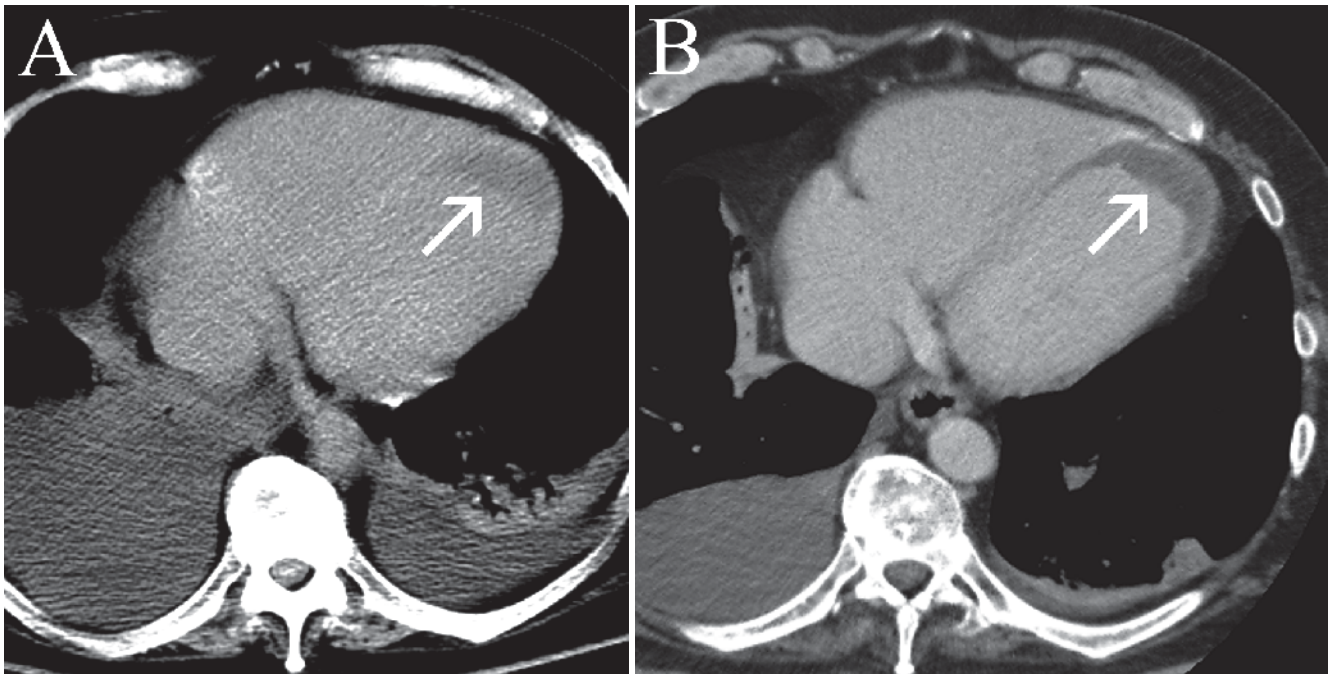
Figure 15.7. Sixty-two-year-old male admitted with a recent myocardial infarction with a hypoattenuating left ventricular thrombus. A transverse, noncontrast view (**a**) obtained to evaluate the extent of pleural effusion demonstrates an area of low attenuation at the left ventricular apex (*white arrow*). A thrombus was suspected. A repeat scan 1 week later obtained with a small amount of intravenous contrast (**b**) demonstrates clear delineation of the large thrombus at the left ventricular apex (*white arrow*).
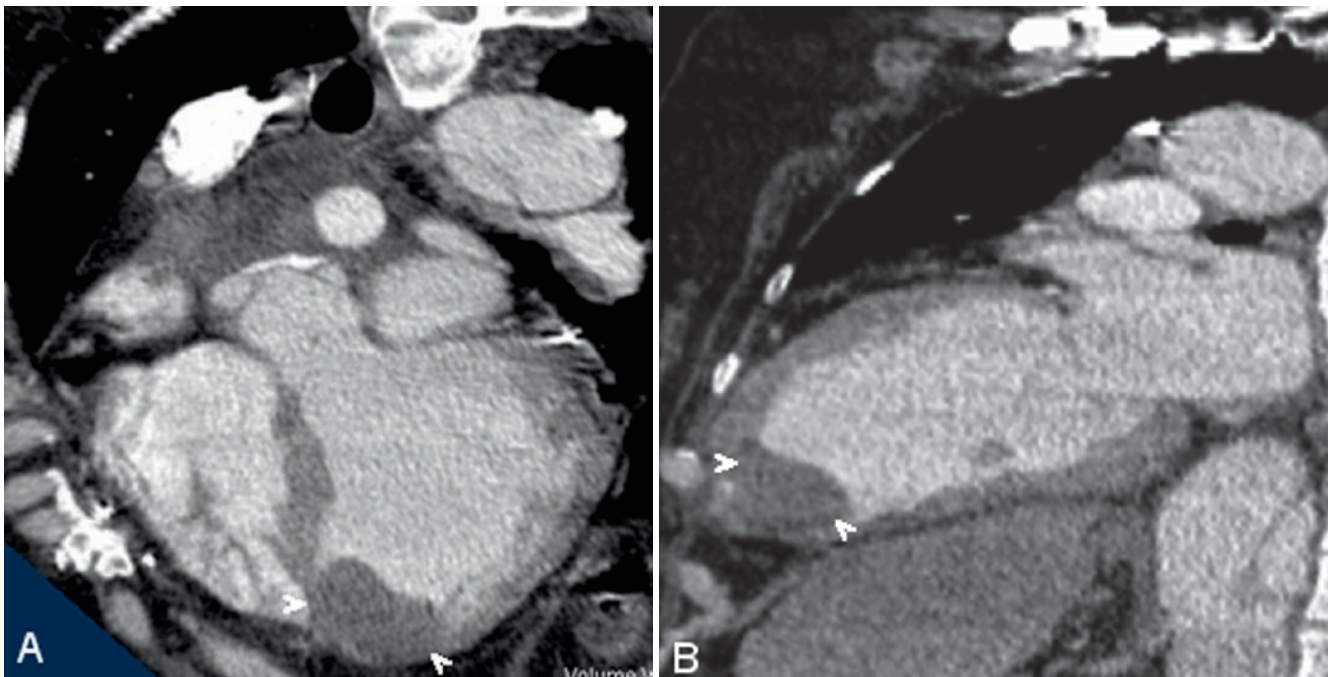

Figure 15.8. Forty-five-year-old woman with a recent myocardial infarction. Four-chamber (**a**) and two-chamber (**b**) views from a cardiac CT show a left ventricular apical aneurysm with thrombus (*white arrowheads*).

have been reported in up to one third of transmural infarctions [30], and are associated much more commonly with apical and anterior infarctions, in comparison to inferior wall infarctions [30, 31]. Visualization of multiple thrombi is not uncommon in the postinfarction setting.

Atrial thrombi can be very problematic to confidently diagnose. Patients at risk for having atrial thrombi commonly have enlarged atria with heterogeneous enhancement as a result of circulatory stasis within the left atrium. This smoke-like enhancement can be especially prominent in the left atrial appendage, and, in patients with severe atrial enlargement, poor opacification of the chamber and appendage may make exclusion of thrombus very difficult (Figure 15.10). As a result, TEE is still considered
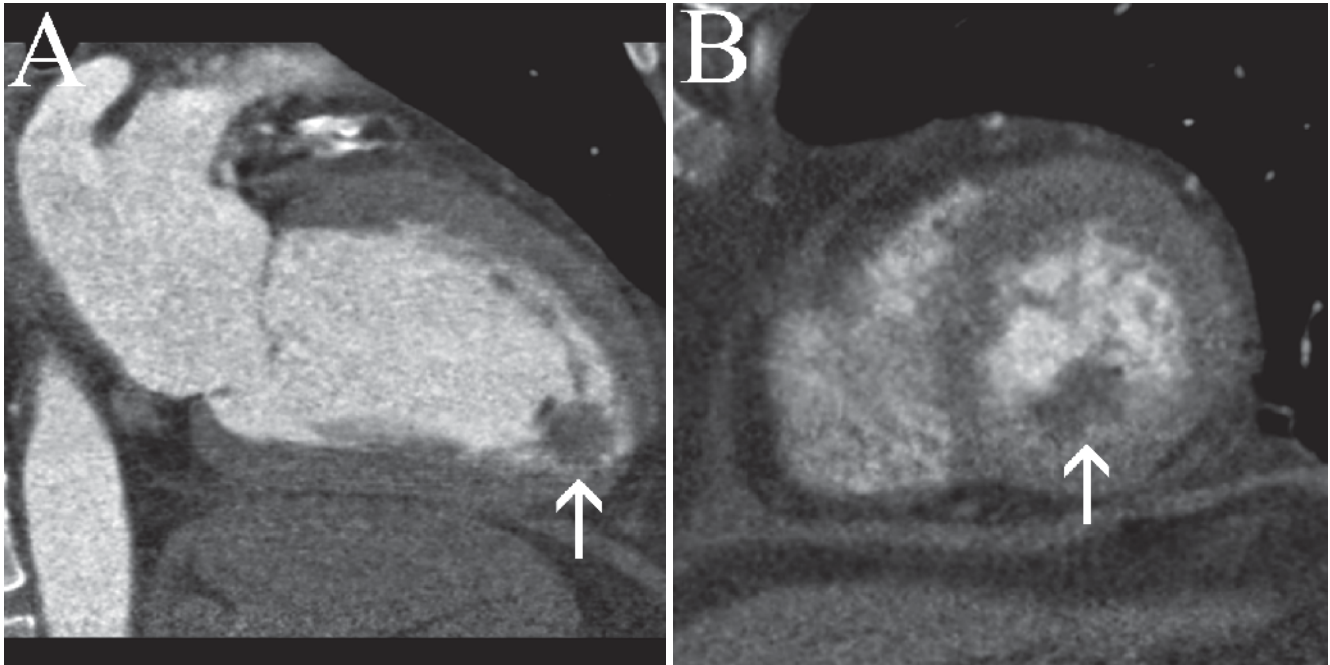
Figure 15.9. Fifty-five-year-old male with a mass at the ventricular apex on transthoracic echocardiogram. Images from a cardiac CT scan obtained in the two-chamber (**a**) and short axis (**b**) planes are shown. A mobile, intracameral, low attenuating, nonenhancing, apical mass is seen consistent with a thrombus. A small area of apical septal late gadolinium enhancement was demonstrated on the patient's CMR (not shown).
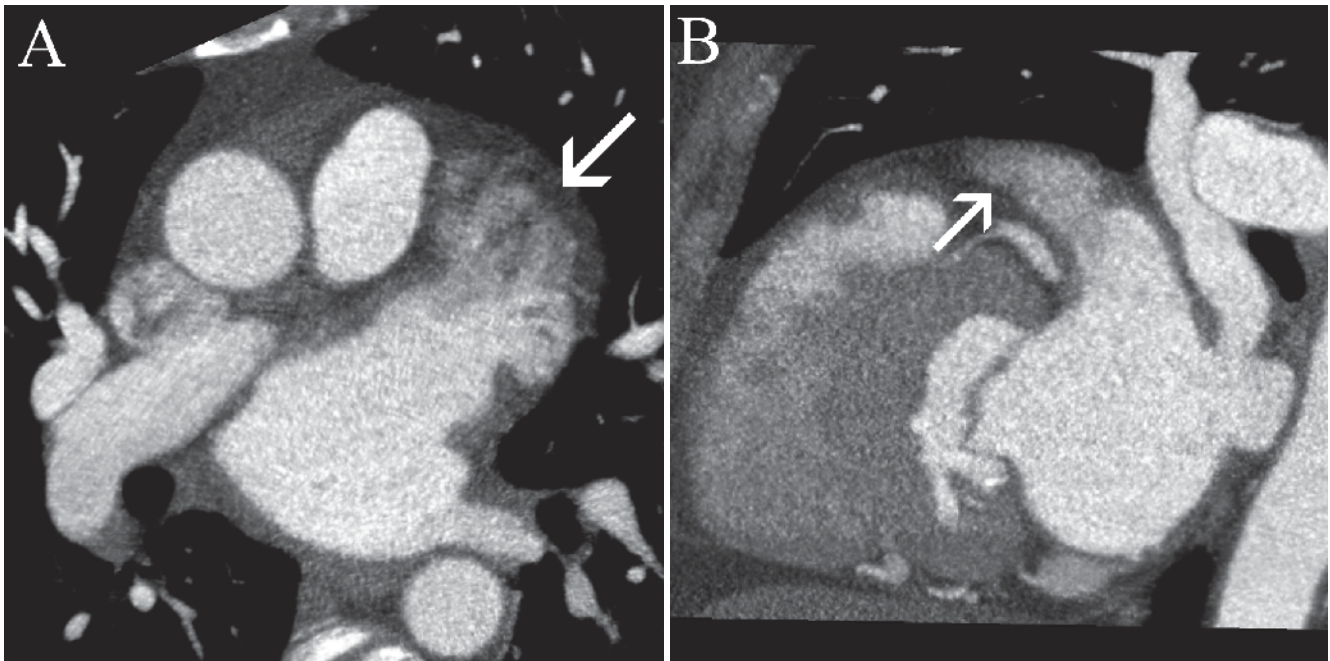

Figure 15.10. Forty-seven-year-old female with atypical chest pain. Orthogonal MPR views of the left atrium from a CCTA (**a**, **b**) demonstrate left atrial enlargement with heterogeneous enhancement of the left atrial appendage. No thrombus was identified on echocardiography. Heterogeneous opacification of the left atrial appendage is a significant pitfall in the identification or exclusion of atrial thrombi on CCTA.

the gold standard for the evaluation of a thrombus in the left atrium or left atrial appendage. Imaging protocols with a delayed phase or with the patient in the prone position have been reported as techniques for improved opacification of the atrial appendage, although these techniques are not yet widely employed [32, 33]. When a nonenhancing filling defect is clearly delineated by contrast, however, a left atrial appendage thrombus can be more easily diagnosed (Figure 15.11). Differentiation from other cardiac masses is usually made on the clinical basis in patients with known atrial enlargement and dysfunction. Right atrial thrombi may form in the atrial appendage, and can be difficult to delineate due to the inherently homogeneous opacification of the normal right heart (Figure 15.12). There are however lower risks of thrombus development in the right atrial appendage, since this structure tends to be flatter and more
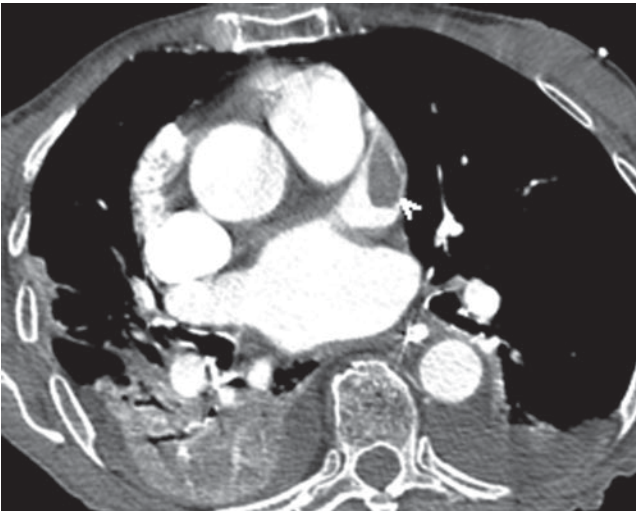
Figure 15.11. Forty-eight-year-old female with left atrial enlargement and atrial fibrillation. On a contrast-enhanced CT scan, a filling defect is clearly identified in the left atrial appendage (*white arrowhead*). When such a defect is clearly delineated by contrast as in this case, thrombus can be more definitively identified.

broad-based, compared to the left atrial appendage, which is a more lobulated or tubular structure and has a neck. These morphologic differences make the left atrial appendage more prone to the development of thrombi compared to the right atrial appendage.

Metastatic Disease

Metastatic lesions are the most common cause of a neoplastic mass in the heart. Metastatic disease has been reported as more common in the right heart, but this may

be due to the earlier recognition of metastatic lesions in the right ventricle, since the wall is thinner than that of the left ventricular wall. Most metastatic lesions are isoattenuating to the myocardium on precontrast CT imaging. Contrast enhancement of metastatic lesions is somewhat variable depending on the degree of vascularity of the neoplasm. Most metastases enhance less than the myocardium initially after administration of contrast, but will slowly accumulate and retain contrast. Metastases may also show retention of contrast on late-phase imaging. This pattern of enhancement may be less well-characterized on CT, since multiphasic imaging with CT is uncommonly performed (Figure 15.13). It should also be noted that the optimal phase for CCTA during coronary arterial enhancement is earlier than the optimal phase for demonstrating myocardial wall enhancement. As a result, the differential enhancement between a metastatic lesion and normal myocardium may not be as clearly seen on CCTA (Figure 15.14). The most common morphology of cardiac metastatic disease is an intramural mass or a mass with a broad-based attachment, in contradistinction to benign masses, which tend to be intracameral and have a narrow attachment. Many metastases which invade the heart from the adjacent mediastinal or pericardial spaces may, however, involve the epicardium first, and subsequently invade into the myocardium. Metastatic disease to the heart is found in up to 10% of patients with a primary at the time of autopsy [34]. Although numerous primary tumor sites have been reported to be metastatic to the heart, the lung is the most common site of a primary tumor, occurring in up to 36.7% of patients [35]. Melanoma is, however, an important source of hematogenous disease to the heart from a distant primary site that does not first involve the
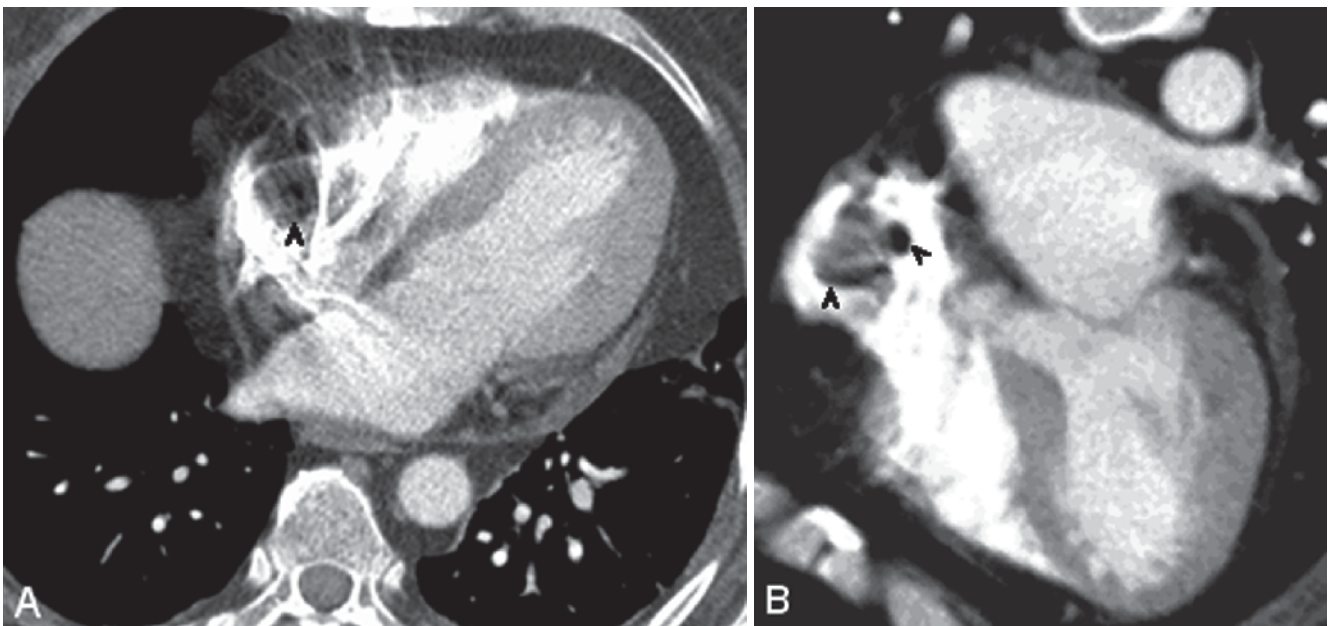

Figure 15.12. Thirty-eight-year-old female with recent resection of gastric carcinoma. Transverse (**a**) and four-chamber (**b**) views are shown from a CT scan of the chest. There is some heterogeneous opacification of the right atrium with some streaking, although the thrombus can be seen through these artifacts (*black arrowheads*). The patient also had a large parenchymal hepatic hematoma, related to her recent surgery, which may have contributed to the development of a right atrial thrombus. CMR (not shown) showed features consistent with a thrombus, and this structure resolved on subsequent studies.
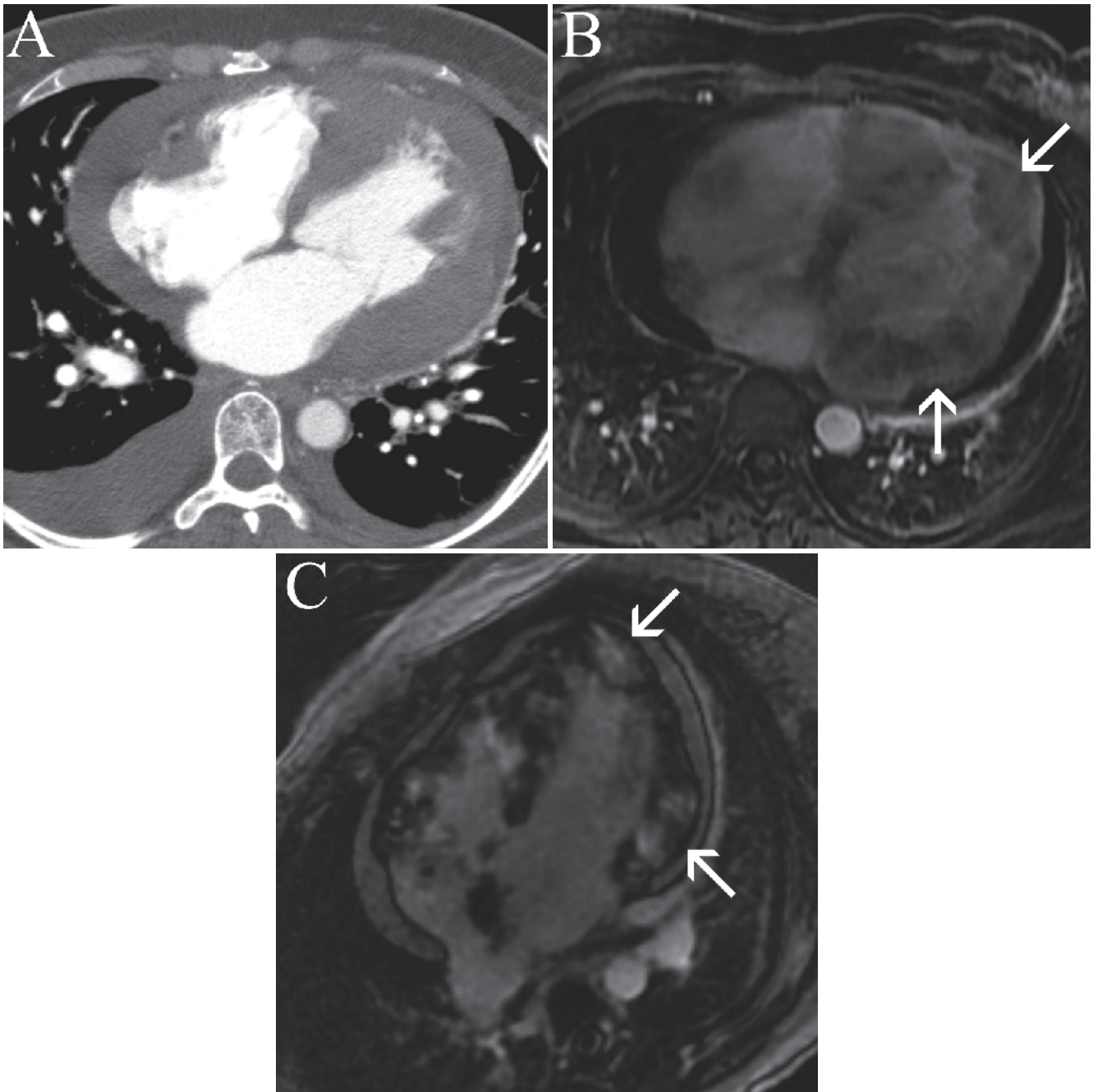
Figure 15.13. Forty-five-year-old female with metastatic melanoma. A transverse view from a contrast-enhanced CT scan (**a**) shows irregular thickening of the ventricular walls and a moderate-sized pericardial effusion. The ventricular metastases are not well-delineated due to the early phase of contrast administration, which was in part, due to the patient's poor cardiac function. A postcontrast CMR sequence obtained at 70 s after intravenous injection of gadolinium (**b**) demonstrates areas of relatively decreased enhancement related to the perfused myocardium (*white arrows*). A delayed, four-chamber view obtained 10 min after contrast administration (**c**) demonstrates late enhancement within the cardiac metastases (*white arrows*).

mediastinum [36]. An example of metastases involving the right ventricle is shown in Figure 15.15.

Myxomas

Myxomas are the most common benign neoplasm of the heart and comprise 50% of all primary cardiac masses. Myxomas characteristically occur in the atrial, and are more commonly left atrial rather than right atrial, with a reported predominance of 80% compared to 20% in the right atrium. Masses which arise in the atria may also prolapse into the ventricular chambers [14]. Myxomas have also, however, been reported to occur in both ventricles. The most common imaging appearance is that of a lobulated mass with precontrast hypoattenuation relative to blood pool and relative to myocardium. Masses are commonly lobulated in appearance and predominantly intracameral. The most common site of attachment for either right or left atrial myxomas is at the fossa ovalis, which can
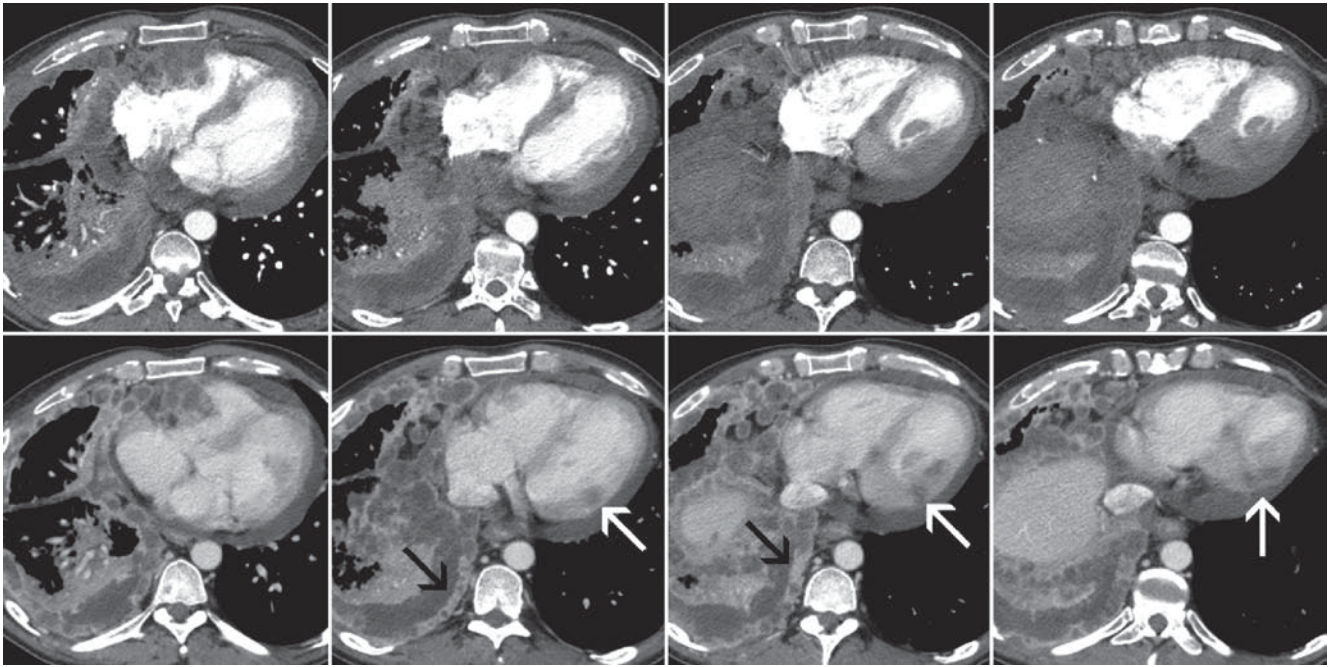
Figure 15.14. Fifty-six-year-old male with high-grade urothelial malignancy and cardiac metastases. Transverse views from an arterial phase of a postcontrast CT scan (*top row*) faintly show metastases to the left ventricular myocardium (*white arrows*). These areas of hypoenhancement are better seen in the portal venous phase images (*bottom row*), where the myocardium is more well-enhanced. Note that other metastases are also better seen on the later phase study, including pleural metastases (*black arrows*).
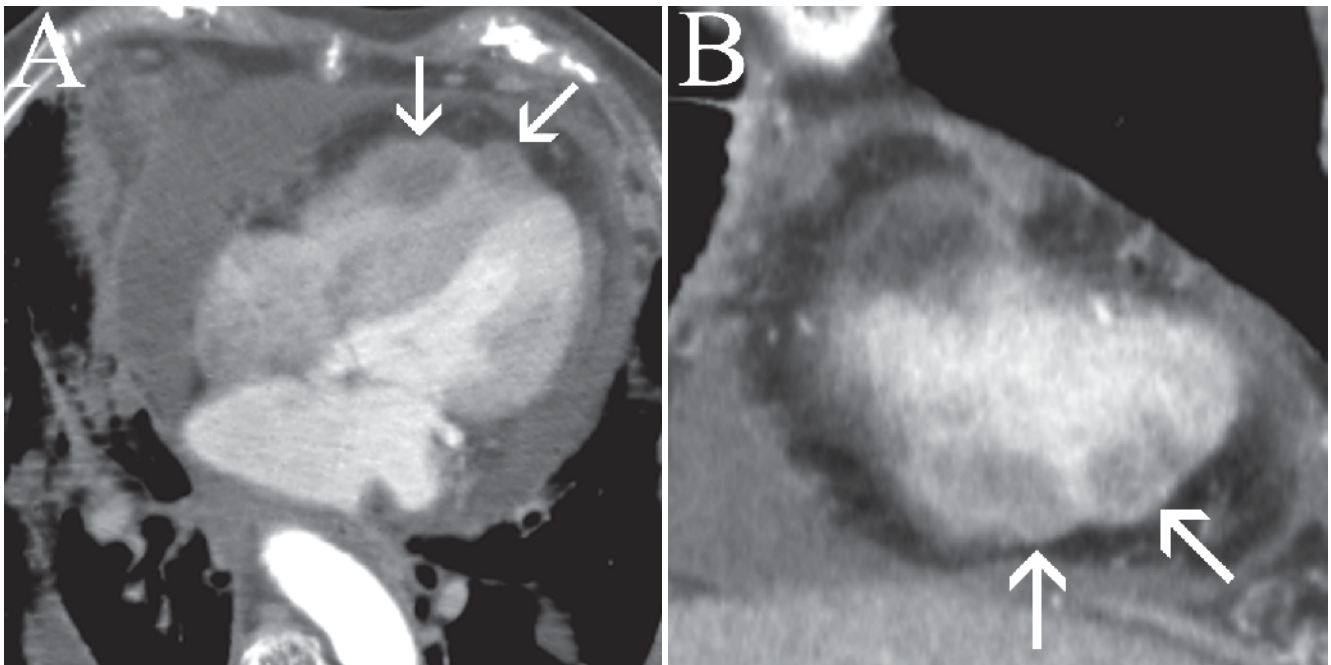

Figure 15.15. Forty-eight-year-old female with right ventricular metastases due to thymic carcinoma. Transverse (**a**) and coronal (**b**) views from a postcontrast CT scan show large masses arising from the wall of the right ventricle, with broad-based attachments to the ventricular wall, consistent with metastatic disease.

be helpful in arriving at the correct diagnosis [9]. Correct identification of the site of attachment is also helpful in presurgical planning. Atrial myxomas commonly demonstrate punctate or coarse calcifications, which is also useful in establishing the diagnosis. Precontrast hypoattenuation is commonly seen relative to blood pool and normal myocardium (Figure 15.16). Rarely, atrial myxomas may be diffusely and densely calcified [17].

The classic triad of clinical symptoms reported with myxomas includes constitutional symptoms, manifestations of obstructive valvular disease, and embolic phenomenon. Constitutional symptoms include fever, malaise, weight loss, and anemia, among others. These symptoms are likely related to an autoimmune response, initiated by the tumor [37]. Cardiac-related symptoms of atrial myxomas vary depending on the chamber of involvement. Atrial
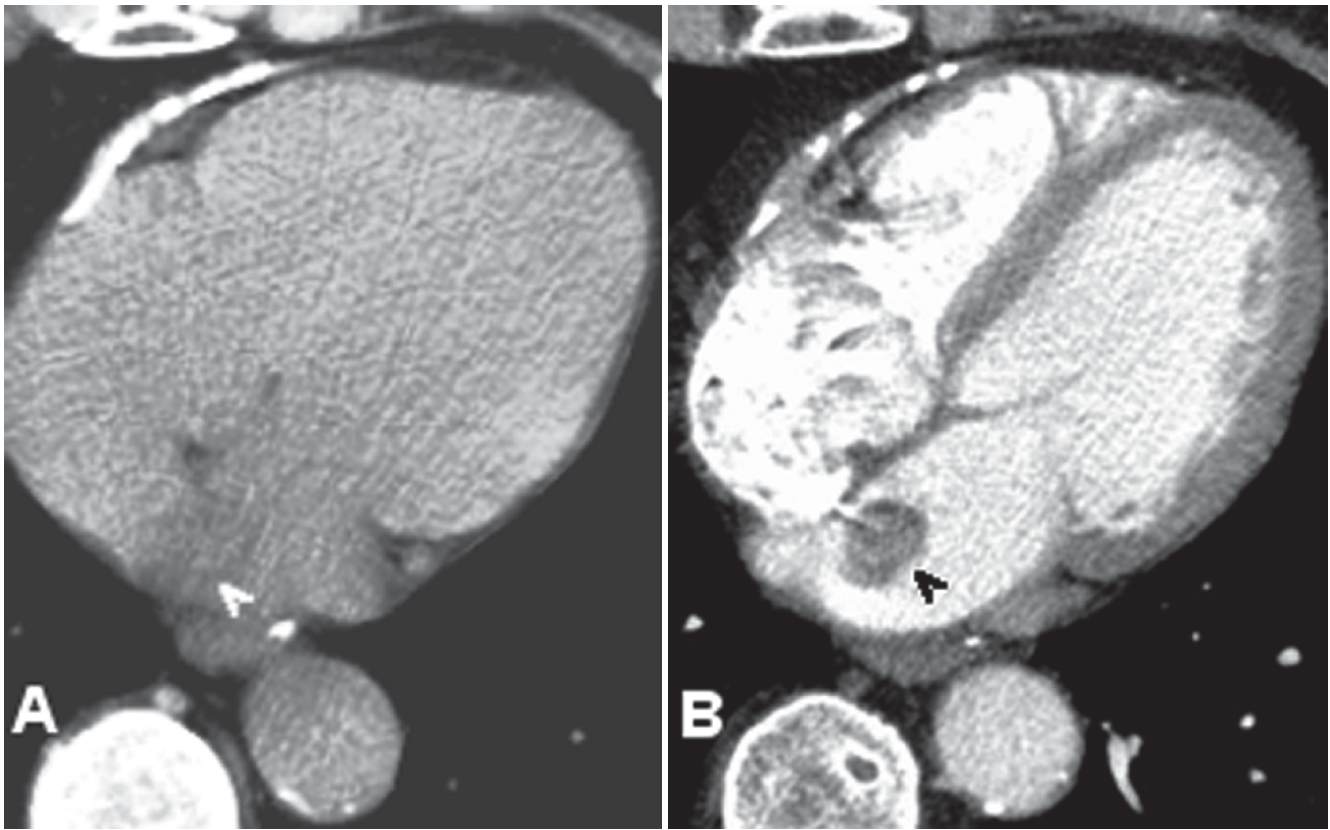
Figure 15.16. Fifty-two-year-old male with a left atrial mass. A precontrast CT scan (**a**) demonstrates the low attenuation left atrial mass. The postcontrast study (**b**) shows no enhancement, and delineates the pedunculated nature of the mass, which arises from the region of the fossa ovalis, consistent with left atrial myxoma.

myxomas have been commonly reported to mimic mitral valve disease and rheumatic heart disease by clinical presentation [38]. Involvement of other valves may, however, produce manifestations of aortic, pulmonic, or tricuspid valvular disease. Embolization is another common feature of myxomas, and may occur to either the pulmonic or systemic circulation, depending on the chamber of involvement. Up to 35% of left atrial myxomas and up to 10% of right atrial myxomas may develop emboli, although this difference could be related to the more apparent manifestations of systemic emboli [39].

A genetic predisposition to myxomas has been postulated and suggested by case reports of families with multiple members with myxomas and in patients with several myxomas [40]. Notably, Carney's Syndrome may be associated with atrial myxomas in two thirds of patients in addition to other manifestations including mammary myxoid fibroadenomas, pigmented cutaneous lesions, endocrine disorders, testicular tumors, and schwannomas [41].

Cardiac Sarcomas

Cardiac sarcomas comprise the most common primary malignant tumors of the heart, but are a rare entity overall, with a prevalence at autopsy as low as 0.0001% [42]. Metastases to the heart outnumber malignant primary lesions by 20–40

to 1. Among subtypes of sarcoma, angiosarcomas are most common, comprising approximately 37%. This tumor subtype in particular tends to occur commonly in the right atrium. Other subtypes tend to arise most commonly from the left atrium, although all types of sarcomas may occur in any chamber [13]. For most cardiac sarcomas, survival is reported as very poor, with metastases commonly detected shortly after clinical presentation [10].

On CCTA and CMR, angiosarcomas may show areas of hemorrhage and necrosis and may appear heterogeneous. Avid enhancement is commonly seen (Figure 15.17), and tumors may be difficult to delineate from the ventricular chamber on later phases due to bright enhancement. Venous lakes and linear vascular structures within masses may be seen, resulting in what has been likened to a "sunray pattern" [43]. Two morphological appearances of angiosarcomas have been reported, including a focal mass arising from the myocardium itself or a diffuse infiltrating process involving the myocardium and pericardium [44, 45]. Undifferentiated sarcomas are tumors with no specific histological staining patterns. The nature and definition of tumors in this category has changed over time as histological techniques have improved. Similar to angiosarcomas, these tumors may either present as a focal mass or as a diffusely infiltrative myocardial and pericardial process. The common site of origin is the left atrium, with a predisposition reported at 80% [13]. A propensity for valvular
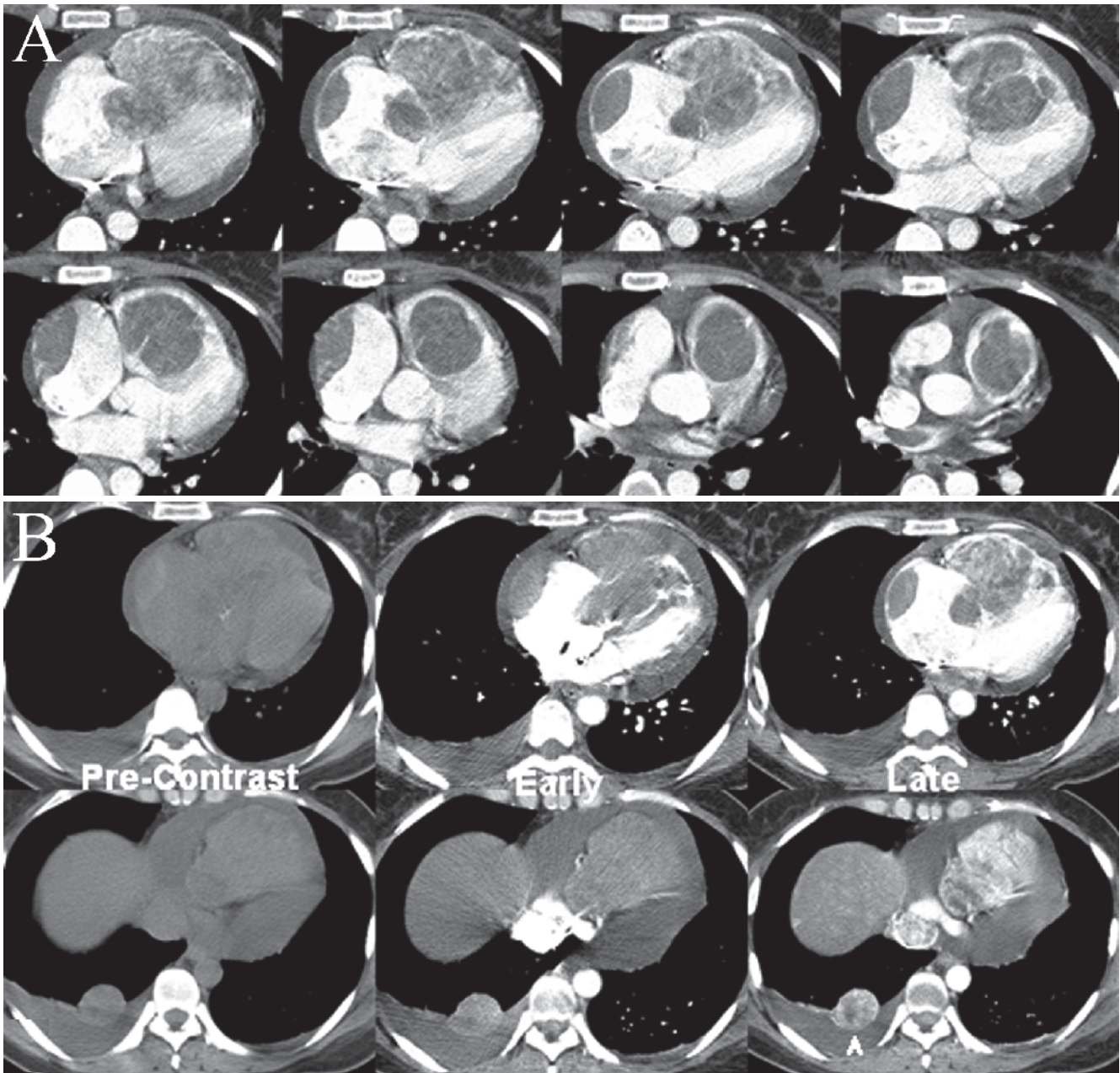
Figure 15.17. (**a, b**) Thirty-three-year-old female with angiosarcoma. Sequential precontrast, early, and late contrasted images demonstrate vascular enhancement within the angiosarcoma. Note the enhancing right lower lobe pulmonary nodule (*arrowhead*), consistent with a metastasis.

involvement has also been reported [46–48]. Rhabdomyosarcomas are very uncommon in adults, but are the most common form of cardiac sarcomas and the most common primary cardiac malignancy in pediatric populations [13]. Embryonal rhabdomyosarcomas occur in pediatric patients, whereas tumors in adults tend to be more pleomorphic [49]. Osteosarcomas of the heart are rare neoplasms, and are distinguished by their propensity to form dense calcifications [50], although some tumors of this type may demonstrate only minimal calcification [13]. Other tumor subtypes include leiomyosarcoma, fibrosarcoma, and liposarcoma, although these are even rarer than the aforementioned neoplasms.

Cardiac Lymphoma

Cardiac lymphoma is a very rare entity, and in a series of 533 cardiac tumors and cysts, it accounted for only 1.3% of tumors [11]. These tumors are rare since there are no true intracardiac lymph nodes. Tumors likely arise from primitive, totipotential mesenchymal cells, and usually consist of high grade B-cell lymphoma. Strictly defined, cardiac lymphoma includes lymphoma involving the heart and pericardium without other areas of lymphomatous involvement. Anecdotal reports suggest that there is increased risk for cardiac lymphoma in AIDS and in other immune deficiency states [51]. Given the rarity of this entity, the radiologic

findings are not well-established, although reports indicate that tumors are usually relatively isoattenuating on CT and isointense on CMR, with heterogeneous enhancement after contrast administration [52].

Lipoma

Cardiac lipomas are the second most common cause of a benign cardiac neoplasm, after myxomas. Lipomas are easily recognized as benign by the homogeneous, precontrast attenuation consistent with fat, which demonstrate essentially no enhancement after contrast administration. Tumors are soft and may be large at the time of initial diagnosis. Symptoms are usually due to mass effect, although commonly cardiac lipomas are detected incidentally and prior to onset of clinical manifestations. Some tumors may encase coronary arteries, resulting in mass effect and displacement, making resection difficult [53]. Although there is seldomly diagnostic uncertainty, some entities may mimic lipomas, including lipomatous hypertrophy of the interatrial septum (Figure 15.18). Rarely, lipomatous metaplasia within chronic myocardial infarctions may be misdiagnosed as a lipoma [54].

Papillary Fibroelastoma

Papillary fibroelastomas, also known as Lambl excrescences, are avascular masses comprised of fronds of dense connective tissue. These masses may be either reactive in nature or may be related to a hamartoma [55]. The true prevalence of this entity is not known, and these tumors have been postulated to be under-recognized and under-diagnosed due to their small size. Most sources refer to these lesions as the third most common benign neoplasms behind myxomas and lipomas. Ninety percent of papillary fibroelastomas occur on the valves, with the aortic valve being the most common location. When associated with the atrioventricular valves, these tumors tend to occur along the atrial side, which may help to differentiate these lesions from thrombi [56]. Associated valvular dysfunction is common, although many of these lesions are detected incidentally [57]. An additional, common presentation is embolic phenomenon, which may occur to the systemic or pulmonary circulation [58]. These tumors are, however, uncommonly reported on CCTA, and as a result no characteristic CCTA features of this entity have emerged.

Pediatric Cardiac Masses

In pediatric patients who present with cardiac masses, a separate set of diagnostic possibilities should be considered. Pediatric patients will less commonly present for CCTA evaluation, due to radiation concerns. Additionally, since there is sparse literature on CCTA in pediatric patients, the typical appearances of many masses are difficult to delineate. However, some familiarity with masses which may present in pediatric patients is useful to physicians involved in cardiac imaging.

In infants and children, the most common masses encountered are rhabdomyomas. These masses tend to be in the wall of the ventricles, and the vast majority of these masses are multiple. A strong association with tuberous sclerosis is present, although many patients do not manifest other signs of tuberous sclerosis until many years later. Spontaneous regression of tumors is common, although
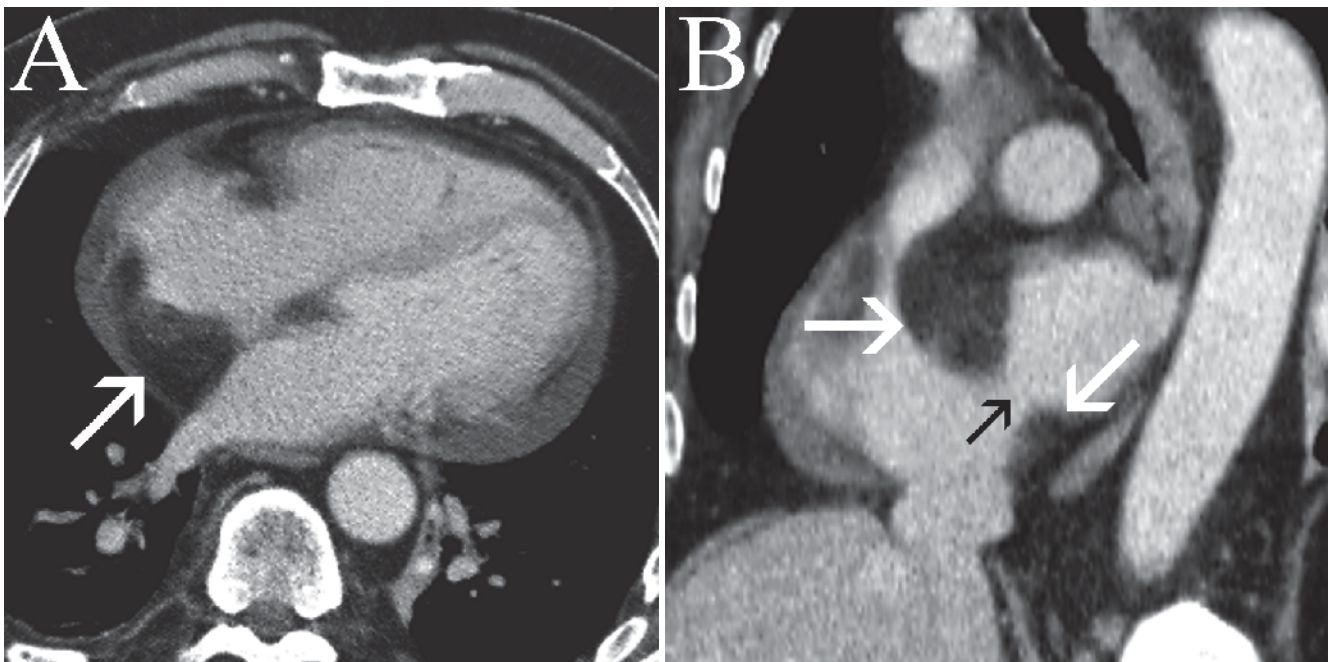

Figure 15.18. Seventy-eight-year-old male with lipomatous hypertrophy of the interatrial septum. Images from a CT scan of the chest obtained in the transverse plane (**a**) and in the short axis plane of the heart (**b**) show lipomatous hypertrophy in the wall of the interatrial septum (*white arrows*). Note the characteristic sparing of the region of the fossa ovalis (*black arrow*).

the initial clinical presentation may be severe [59]. Cardiac fibroma constitutes the second most common mass in the heart, and is usually seen as a large, solitary mass. Some of these may grow to an enormous size. Symptoms may include heart failure, chest pain, arrhythmias, and sudden cardiac death [60]. Myxomas are very rare in the pediatric population, but have been reported in large series in older pediatric patients and adolescents [17]. As described earlier, the most common malignant neoplasm in pediatric patients is a cardiac rhabdomyosarcoma, which often has embryonal features at histology. Additional rare tumors are encountered in pediatric populations including cardiac angiomas, cardiac teratomas, and Purkinje cell tumors.

Mimics of Cardiac Masses

Several normal structures in the heart may mimic a mass even to an experienced reader. Misidentification of normal structures as masses can lead to unnecessary biopsies, surgeries, and subsequent morbidity. Notably, in the right atrium, a prominent crista terminalis may mimic a cardiac mass. When a small and reticulated mass is present along this structure in the right atrium, a network of Chiari may be present. Uncommonly, prominence of the Eustachian valve or juxtacaval lipomatous tissue may mimic a lower right atrial mass. Usually, the contrast timing for the right ventricle is such that some saline is being injected at the time of scanning of the heart. However, in some cases, unopacified blood flow entering the right atrium from the inferior vena cava may simulate a mass when the right atrium is otherwise filled with contrast. In the left atrium, the "coumadin ridge," located between the atrial appendage ostium and the superior pulmonary vein, may appear mass-like.

References

1. Desjardins B, Kazerooni EA. ECG-gated cardiac CT. *Am J Roentgenol*. 2004;182:993–1010.
2. Newhouse JH, Murphy RX. Tissue distribution of soluble contrast: effect of dose variation and changes with time. *Am J Roentgenol*. 1981; 136:463–467.
3. Cademartiri F, Mollet N, van der Lugt A, et al. Non-invasive 16-row multislice CT coronary angiography: usefulness of saline chaser. *Eur Radiol*. 2004;14:178–183.
4. Awai K, Hiraishi K, Hori S. Effect of contrast material injection duration and rate on aortic peak time and peak enhancement at dynamic CT involving injection protocol with dose tailored to patient weight. *Radiology*. 2004;230(1):142–150.
5. Cademartiri F, Nieman K, van der Lugt A, et al. Intravenous contrast material administration at 16-detector row helical CT coronary angiography: test bolus versus bolus-tracking technique. *Radiology*. 2004;233:817–823.
6. Bae KT, Tran HQ, Heiken JP. Uniform vascular contrast enhancement and reduced contrast medium volume achieved by using exponentially decelerated contrast material injection method. *Radiology*. 2004; 231:732–736.
7. Boyd DB. Computerized transmission tomography of the heart using scanning electron beams. In: Higgins CH, ed. *Computed Tomography of the Heart and Great Vessels*. Mount Kisco, New York: Futura; 1983:45–55.
8. Newhouse JH. Fluid compartment distribution of intravenous iothalamate in the dog. *Invest Radiol*. 1977;12:364–367.
9. Prichard RW. Tumors of the heart. *Arch Pathol*. 1951;51:98–128.
10. Glancy DL, Morales JB, Roberts WC. Angiosarcoma of the heart. *Am J Cardiol*. 1968;21:413–419.
11. McAllister HA, Fenoglio JJ Jr. *Tumors of the Cardiovascular System: Atlas of Tumor Pathology, Second Series*. Washington, DC: Armed Forces Institute of Pathology; 1978.
12. Lund JT, Ehman RL, Julsrud PR, et al. Cardiac masses: assessment by MR imaging. *AJR Am J Roentgenol*. 1989;152(3):469–473.
13. Burke AP, Cowan D, Virmani R. Primary sarcomas of the heart. *Cancer*. 1992;69:387–395.
14. Tazelaar HD, Locke TJ, McGregor CG. Pathology of surgically excised primary cardiac tumors. *Mayo Clin Proc*. 1992;67(10):957–965.
15. Lam KY, Dickens P, Chan AC. Tumors of the heart. A 20-year experience with a review of 12,485 consecutive autopsies. *Arch Pathol Lab Med*. 1993;117(10):1027–1031.
16. Marx GR. Cardiac tumors. In: Emmanouilides GC, Gutgesell HP, Riemenschneider TA, Allen HD, eds. *Moss and Adams Heart Disease in Infants, Children, and Adolescents: Including the Fetus and Young Adult*. 5th ed. Vol 2. Baltimore: Williams & Wilkins; 1995:1773–1786.
17. Burke A, Virmani R. *Tumors of the Heart and Great Vessels: Atlas of Tumor Pathology*. Fasc 16, ser 3. Washington, DC: Armed Forces Institute of Pathology; 1996.
18. Takach TJ, Reul GJ, Ott DA, Cooley DA. Primary cardiac tumors in infants and children: immediate and long-term operative results. *Ann Thorac Surg*. 1996;62(2):559–564.
19. Ludomirsky A. Cardiac tumors. In: Bricker JT, Fisher DJ, eds. *The Science and Practice of Pediatric Cardiology*. 9th ed. Vol 2. Baltimore: Williams & Wilkins; 1998:1885–1893.
20. Araoz PA, Eklund HE, Welch TJ, Breen JF. CT and MR imaging of primary cardiac malignancies. *Radiographics*. 1999;19(6):1421–1434.
21. Chiles C, Woodard PK, Gutierrez FR, Link KM. Metastatic involvement of the heart and pericardium: CT and MR imaging. *Radio-Graphics*. 2000;20:1073–1103.
22. Grebenc ML, Rosado de Christenson ML, Burke AP, Green CE, Galvin JR. Primary cardiac and pericardial neoplasms: radiologic–pathologic correlation. *Radiographics*. 2000;20:1073–1103; quiz 1110–1071;1112.
23. Grebenc ML, Rosado-de-Christenson ML, Green CE, Burke AP, Galvin JR. Cardiac myxoma: imaging features in 83 patients. *Radiographics*. 2002; 2(3):673–689.
24. Piazza N, Chughtai T, Toledano K, et al. Primary cardiac tumours: eighteen years of surgical experience on 21 patients. *Can J Cardiol*. 2004; 20(14):1443–1448.
25. Tatli S, Lipton MJ. CT for intracardiac thrombi and tumors. Int J Cardiovasc Imaging 2005;21(1):115–131.
26. Butany J, Nair V, Naseemuddin A, et al. Cardiac tumours: diagnosis and management. *Lancet Oncol*. 2005;6(4):219–228.
27. Leipsic JA, Heyneman LE, Kim RJ. Cardiac masses and myocardial diseases. In: McAdams HP, Reddy GP, eds. *Cardiopulmonary Imaging Syllabus – 2005*. Leesburg, VA: American Roentgen Ray Society; 2005: 1–13.
28. Sparrow PJ, Kurian JB, Jones TR, Sivananthan MU. MR imaging of cardiac tumors. *Radiographics*. 2005;25:1255–1276.
29. Barkhausen J, Hunold P, Eggebrecht HH, et al. Detection and characterization of intracardiac thrombi on MR imaging. *AJR*. 2002;179: 1539–1542.
30. Weinreich DJ, Burke JF, Ferrel JP. Left ventricular mural thrombi complicating acute myocardial infarction long-term follow-up with serial echocardiography. *Ann Intern Med*. 1984;100(6):789–794.
31. Asinger RW, Mikell FL, Elsperger J, Hodges M. Incidence of left ventricular thrombosis after acute transmural myocardial infarction: serial evaluation by two-dimensional echocardiography. *NEJM*. 1981; 305(6):297–302.
32. Hur J, Kim YJ, Nam JE, et al. Thrombus in the left atrial appendage in stroke patients: detection with cardiac CT angiography–a preliminary report. *Radiology*. 2008;249(1):81–87.
33. Hur J, Kim YJ, Lee HJ, et al. Left atrial appendage thrombi in stroke patients: detection with two-phase cardiac CT angiography

versus transesophageal echocardiography. *Radiology*. 2009;251(3): 683–690.

34. Abraham KP, Reddy V, Gattuso P. Neoplasms metastatic to the heart: review of 3314 consecutive autopsies. *Am J Cardiovasc Pathol*. 1990; 3:195–198.

35. Klatt EC, Heitz DR. Cardiac metastases. *Cancer*. 1990;65:1456–1459.

36. MacGee W. Metastatic and invasive tumours involving the heart in a geriatric population: a necropsy study. *Virchows Arch A Pathol Anat Histopathol*. 1991;419:183–189.

37. Bjessmo S, Ivert T. Cardiac myxoma: 40 years' experience in 63 patients. *Ann Thorac Surg*. 1997;63:697–700.

38. Markel ML, Waller BF, Armstrong WF. Cardiac myxoma: a review. *Medicine*. 1987;66:114–125.

39. Castells E, Ferran V, Octavio-de-Toledo MC. Cardiac myxomas: surgical treatment, long-term results and recurrence. *J Cardiovasc Surg*. 1993;34:49–53.

40. Carney JA. Differences between nonfamilial and familial cardiac myxoma. *Am J Surg Pathol*. 1985;9:53–55.

41. Carney JA, Gordon H, Carpenter PC, Shenoy BV, Go VW. The complex of myxomas, spotty pigmentation and endocrine overactivity. *Medicine*. 1985;64:270–283.

42. McCallister HA Jr. Primary tumors of the heart and pericardium. *Curr Probl Cardiol*. 1979;4:1–51.

43. Yahata S, Endo T, Honma H, et al. Sunray appearance on enhanced magnetic resonance image of cardiac angiosarcoma with pericardial obliteration. *Am Heart J*. 1994;127:468–471.

44. Bruna J, Lockwood M. Primary heart angiosarcoma detected by computed tomography and magnetic resonance imaging. *Eur Radiol*. 1998;8:66–68.

45. Jannigan DT, Husain A, Robinson NA. Cardiac angiosarcomas: a review and a case report. *Cancer*. 1986;57:852–859.

46. Herhusky MJ, Gregg SB, Virmani R, Chun PKC, Bender H, Gray GF Jr. Cardiac sarcoma presenting as metastatic disease. *Arch Pathol Lab Med*. 1985;109:943–945.

47. Ludomirsky A, Vargo TA, Murphy DJ, Gresik MV, Ott DA, Mullins CE. Intracardiac undifferentiated sarcoma in infancy. *J Am Coll Cardiol*. 1985;6:1362–1364; Abstract 37.

48. Itoh K, Matsumura T, Egawa Y, et al. Primary mitral valve sarcoma in infancy. *Pediatr Cardiol*. 1998;19:174–177.

49. Hwa J, Ward C, Nunn G, et al. Primary interventricular cardiac tumors in children: contemporary diagnostic and management options. *Pediatr Cardiol*. 1994;15:233–237.

50. Chaloupka JC, Fishman EK, Siegelman SS. Use of CT in the evaluation of primary cardiac tumors. *Cardiovasc Intervent Radiol*. 1986;9: 132–135.

51. Holladay AO, Siegel RJ, Schwartz DA. Cardiac malignant lymphoma in acquired immune deficiency syndrome. *Cancer*. 1997;70(8): 2203–2207.

52. Dorsay TA, Ho VB, Roviera MJ, Armstrong MA, Brissette MD. Primary cardiac lymphoma: CT and MR findings. *J Comput Assist Tomogr*. 1993; 17:978–981.

53. Hananouchi GI, Goff WB. Cardiac lipoma: six-year follow-up with MRI characteristics, and a review of the literature. *Magn Reson Imaging*. 1990;8(6):825–828.

54. Banks KP, Lisanti CJ. Incidental finding of a lipomatous lesion involving the myocardium of the left ventricular wall. *AJR*. 2004;182: 261–262.

55. Rubin MA, Snell JA, Tazelaar HD, Lack EE, et al. Cardiac papillary fibroelastoma: an immunohistochemical investigation and unusual clinical manifestations. *Mod Pathol*. 1995;8:402–407.

56. Klarich KW, Enriquez-Sarano M, Gura GM, et al. Papillary fibroelastoma: echocardiographic characteristics for diagnosis and pathologic correction. *J Am Coll Cardiol*. 1997;30:784–790.

57. Edward FH, Hale D, Cohen A, et al. Primary cardiac valve tumors. *Ann Thorac Surg*. 1991;52:1127–1131.

58. McFadden PM, Lacy JR. Intracardiac papillary fibroelastoma: an occult cause of embolic neurologic deficit. *Ann Thorac Surg*. 1987;43: 667–669.

59. Bosi G, Lintermans JP, Pellegrino PA, et al. The natura history of cardiac rhabdomyoma with and without tuberous sclerosis. *Acta Pediatr*. 1996;85:928–931.

60. Turi GK, Albala A, Fenoglio JJ Jr. Cardiac fibromatosis: an ultrastructural study. *Hum Pathol*. 1980;11:577–579.